ARMY RESEARCH LABORATORY

**AL**

# Correlations between Global Positioning System and U.S. Naval Observatory Master Clock Time

by Thomas B. Bahder

ARL-TR-1282                                                                 June 1997

*19970618 018*

DTIC QUALITY INSPECTED 4

ARL-TR-1282 June 1997

# Correlations between Global Positioning System and U.S. Naval Observatory Master Clock Time

Thomas B. Bahder
Sensors and Electron Devices Directorate

# Abstract

The U.S. Naval Observatory Master Clock is used to steer Global Positioning System (GPS) time. Time-transfer data consisting of the difference between the Master Clock time and the GPS time were recorded from all satellites in the GPS constellation over a time period covering 10 October to 12 December 1995. A Fourier analysis of these data shows a distinct peak in the Fourier spectrum, corresponding approximately to a one-day period. For a more accurate determination of this period, correlations are computed between successive days of data. An average of 25 correlation functions shows a correlation equal to 0.52 at a delay time of 23 hr 56 min (which corresponds to twice the average GPS satellite period). This correlation indicates that GPS time, as measured by the U.S. Naval Observatory, is periodic with respect to the Master Clock, with a period of 23 hr and 56 min. An autocorrelation of a five-day segment of data indicates that these correlations persist for four successive days.

# Contents

# Figures

# Tables

# 1. Introduction

The Global Positioning System (GPS) is made up of a constellation of 24 satellites in four orbital planes about the earth [1–4]. Since full operational capability of the GPS was announced, applications of the GPS have grown exponentially as the system's accuracy, global coverage, and reliability were recognized. However, military [5] and civilian [6] GPS users are already requesting position and time-transfer accuracy beyond that of the system's original design requirements [2]. To improve GPS accuracy, we must revisit the basic underpinnings of the system, including basic physics, time transfer/steering techniques, and current algorithms used to operate the GPS. In this work, I investigate correlations in time difference between the official Department of Defense (DoD) reference standard (the U.S. Naval Observatory (USNO) Master Clock) and GPS time, as determined from single satellite time transfer [7–11].

The GPS is based on measurement of the pseudorange, which is the phase of the pseudorandom noise (PRN) code that is broadcast from a satellite [1,12]. This phase corresponds to the time of flight of the signal from satellite to receiver (modulo the code period). The measured pseudorange from four satellites can be used to determine the user's time and position, relative to the known positions of the satellites in the GPS constellation [1]. If all satellite clocks were "perfectly synchronized" with each other [7,10,13–15], and the user's clock were "perfectly synchronized" with the satellite clocks, the light travel time from three satellites would, in principle, provide sufficient information to determine the user's position in three-dimensional space [3,4,16]. In practice, however, there is some offset between the user's clock and each satellite clock. This offset is determined during the measurement process, if pseudorange measurements are made to four or more satellites. Alternatively, if we know the user's position, and we have the correct time (such as given by the USNO Master Clock) then we can obtain from GPS the time difference between our clock and GPS time by acquiring the navigation message (which contains the satellite ephemeris) and by measuring the pseudorange to one satellite [17]. This is the type of measurement that is routinely made by USNO when GPS time is compared to time on the Master Clock [17].

1

The GPS epoch is 0000 UT (midnight) on January 6, 1980. GPS time is not adjusted by the addition of leap seconds and is therefore, offset from Coordinated Universal Time (UTC) by an integer number of seconds, plus some tens of nanoseconds. As of 1 January 1996, GPS time is ahead of UTC by 11 s. The relation between GPS time $t_{GPS}$ and the best estimate of UTC(USNO) as obtained from GPS, $t_{UTC}$, is given by [20,21]

$$t_{UTC} = t_{GPS} - \Delta t_{UTC} \qquad (1)$$

where

$$\Delta t_{UTC} = \Delta t_{LS} + A_0 + A_1(t_{GPS} - t_{RT}) \qquad (2)$$

where $\Delta t_{LS}$ is the integer leap seconds time offset between GPS and UTC time, $t_{RT}$ is the reference time for the UTC data, and $A_0$ and $A_1$ are constants in the navigation message. The UTC(USNO) time scale is kept within approximately 100 ns of the international time standard, UTC, which is published by the Bureau International des Poids et Mesures (BIPM).

The USNO Master Clock is a hydrogen maser that provides the best real-time estimate of the UTC(USNO) time scale. Hydrogen masers are very stable over short time periods, such as a week. USNO's current Sigma Tau hydrogen masers (STSC Model 2010 (1994)) exhibit a time domain maximum instability of $3.0 \times 10^{-15}$ for periods of 1000 to 10,000 s. However, the Master Clock is steered to the UTC(USNO) time scale, which itself is based on an ensemble of dozens of cesium clocks and five to ten hydrogen masers. Consequently, the UTC(USNO) time scale is very stable. Its rate does not change by more than about 100 ps per day, from day to day.

GPS time is steered to UTC(USNO). During the last several years, these times have been kept within a few hundred nanoseconds. However, data from single-frequency receivers indicate that there is a diurnal variation in the time difference between GPS and UTC(USNO) times [18,19]. In this work, I investigate the residuals of differences between UTC(USNO) Master Clock time and GPS time, as seen through individual GPS satellites, after correcting each satellite clock by using the broadcast $a_{f0}$, $a_{f1}$, and $a_{f2}$ parameters and correcting for ionospheric delay (using an algorithm based on L1 and L2 frequencies) [20].

For DoD purposes, the USNO Master Clock is the best real-time source of time for the time scale USNO(UTC). This time scale is a realization of coordinate time on the geoid, in the rotating Earth-centered, Earth-fixed (ECEF)

2

frame of reference [10,11]. As the Master Clock moves through inertial space, its (coordinate) time agrees with the coordinate time on hypothetical coordinate clocks with which it instantaneously coincides in the underlying Earth-centered inertial (ECI) frame of reference (i.e., the rate of coordinate clocks in this ECI frame is set by time on the geoid*). The GPS is intended to keep coordinate time in this ECI frame (modulo leap seconds). Specifically, the GPS time that a satellite provides to a user is intended to be the same as that of a (stationary) coordinate clock in the underlying ECI frame, at the position of the user, having the rate of clocks on the geoid. (Ashby [10] gives a detailed discussion of GPS time as coordinate time.) Ideally, if all facets of the GPS are implemented correctly, and time transfer is performed correctly, the observed difference between the two sources of time—the USNO Master Clock and GPS—should contain only random measurement errors, but no systematic differences.

---

*The ECI frame referred to is not a true inertial frame of reference, as is commonly used in special relativity. This ECI frame is described by a Schwarzschild-like metric with a transformed coordinate time. See Ashby [10].

# 2. Data Analysis

USNO personnel provided me with data consisting of time differences between UTC(USNO) and GPS times, acquired through the Precise Positioning Service (PPS) via P(Y)-code (encrypted precision code). The data were acquired from all satellites in the GPS constellation [22] during 10 October 1995 to 12 December 1995, which corresponds to modified Julian date (MJD) 50000.00553 to 50063.54009. Pseudorange data were collected by a receiver manufactured by Stanford Telecommunications, Inc. (model 5401C, serial number 021); this dual-frequency (L1 and L2) P(Y)-code receiver is used by USNO to monitor GPS time. USNO made the standard two-frequency correction for ionospheric delay [20]. An algorithm internal to the receiver was used to correct for propagation delay through the troposphere. The broadcast ephemeris was used from each satellite in the receiver's time-transfer computation. Furthermore, two other corrections were made: a Sagnac correction for the Earth rotation, and the relativistic "$e \sin E$" correction of the signal emission time due to eccentricity of the satellite orbit [20].

Each satellite in turn was tracked, and time-transfer data were collected every 6 s, over a track period of 780 s (13 min) [22]. A least-squares fit to the 6-s data was done (over the 13-min track period) to obtain one data point, which represents a best estimate of the difference between the USNO Master Clock and GPS time, via the individual satellite, at the given MJD (or fraction thereof). The 13-min track period was chosen so that the entire navigation message would be received; the navigation message, transmitted every 12.5 min, includes the latest ionospheric and UTC information. The data consisted of 5623 points total, corresponding to approximately 89 points per day. The root mean square (RMS) deviations for the 13-minute-track data points were on the order of 2 to 10 ns.

Figure 1 is a plot of the original data, consisting of the time difference between the USNO Master Clock and GPS time versus the MJD. Over the 63 days of data, the time difference varied from approximately −40 to +50 ns. The long-term variation in the data reflects the complicated response of the GPS to time steering, which includes the Kalman filter process (run at the Master
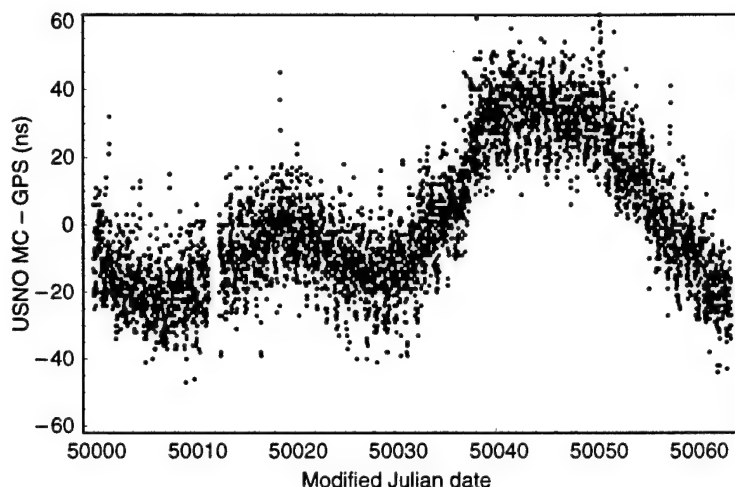
Figure 1: Original data (time difference between USNO Master Clock and GPS time) versus modified Julian date for period MJD 50000.00553 to 50063.54009.

Control Station in Colorado Springs) and the response of other subsystem components. There is a gap in the data during the period MJD 50011.45177 to 50012.46282, due to data acquisition difficulties.

Figure 2 shows a subset of the same data over the time period MJD 50020 to 50028. A salient feature of the data is the scatter of points, on the order of 30 ns peak-to-peak. This scatter is due to a combination of effects [1], including noise in the receiver electronics ($\sim$0.5 m $\approx$ 1.5 ns), multipath effects ($\sim$1.4 m), uncompensated tropospheric delay ($\sim$0.7 m), uncompensated ionospheric delay ($\sim$1.2 m), satellite clock errors ($\sim$2.1 m), and ephemeris errors ($\sim$2.1 m), where all values are $1 - \sigma$ errors in range. The USNO GPS antenna phase center coordinates are believed accurate to approximately 0.5 m. Perhaps the biggest contribution to this scatter in the data arises because the satellites in the constellation do not all have their navigation messages updated at the same time; this variation results in a scatter of values during any given measurement time. Besides this scatter, a diurnal variation is apparent. Figure 3 shows an 11-point average of the data in the time period MJD 50020 to 50028. A diurnal oscillation with a magnitude of 18 to 20 ns peak-to-peak is clearly present. The physical origin of this diurnal variation is not well understood. Workers in the field [18] have proposed a variety of reasons to explain this behavior, including broadcast ephemeris errors, multipath er-
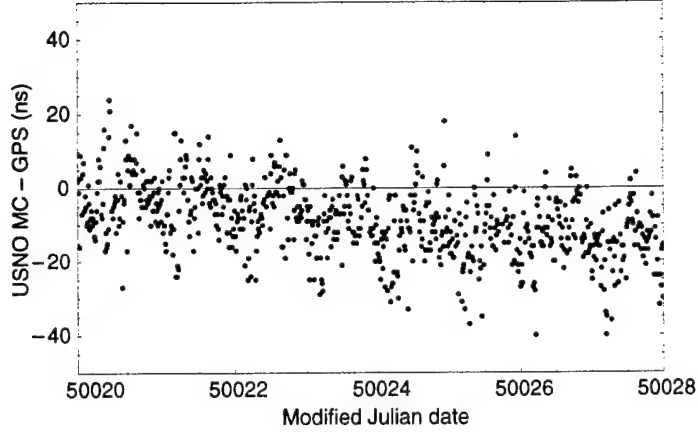
5

Figure 2: Portion of data from MJD 50020 to 50028, on an expanded scale.

rors, incorrect receiver antenna phase center coordinates, the fundamental accuracy limit of the clocks on the Block II satellite vehicles, poor thermal control of the clock systems (on the ground and in the satellites), inaccuracies in modeling of the ionosphere and troposphere, and the possibility that relativistic effects in the GPS have not been accounted for properly.

## 2.1 Fourier Transform

I searched for periodicity in the data by performing a Fourier transform, using a fast Fourier transform (FFT) algorithm. The FFT algorithm [23] requires that the data set be uniformly sampled in time; however, the original data set was not uniformly sampled. Therefore, I fit a cubic spline to the original data set and resampled the data at a uniform sampling rate $\Delta = t_{i+1} - t_i = 0.002$ day, where $t_i$ is the time of the $i$th resampled data point. The sampling rate of the original data varied in the approximate range of 0.009 to 0.013 day, so I have, essentially, lost no information by resampling the data using a smaller sampling interval. For the Fourier transform $H(f)$ of a function $h(t)$, I use the convention

$$H(f_n) = \int_{-\infty}^{+\infty} h(t)e^{2\pi i f_n t}\, dt \approx \Delta \sum_{k=0}^{N-1} h_k e^{2\pi i f_n t_k} = \Delta \sum_{k=0}^{N-1} h_k e^{2\pi i k n} = \Delta\, H_n,$$

(3)

where $h_k = h(t_k)$. For $N$ data points, there are $N$ Fourier amplitudes at frequencies $f_n$, where $n = -N/2, \cdots, 0, \cdots, +N/2$. The finite data set imposes
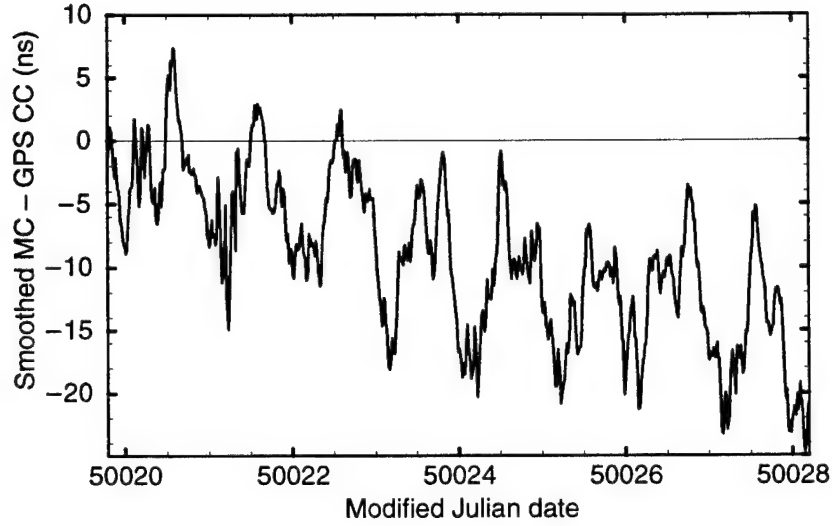
6

Figure 3: Original data, smoothed by taking average of 11 points, from MJD 50020 to 50028. (A diurnal oscillation of (peak-to-peak) magnitude of 18 to 20 ns is evident.)

the periodicity on the amplitudes $H_{n+N} = H_n$. In particular, the amplitudes $H_{-N/2}$ and $H_{N/2}$ are equal, and not independent. Positive frequencies $0 < f < f_c$, where $f_c = 1/(2\Delta)$ is the Nyquist critical frequency, correspond to discrete $f_n$ for $n = 1, 2, \cdots, N/2 - 1$. Furthermore, my data consist of a real function, so the amplitudes for negative frequencies are related to the amplitudes for positive frequencies, $H(-f) = H(f)^*$, or in terms of the discrete amplitudes, $H_{-n} = H_n^*$. Figure 4 shows a plot of the magnitudes of the Fourier transform amplitudes $|H(f_n)|^2$ of the resampled data for the $N/2$ frequencies $f_n$, where $n = 0, 1, \cdots, N/2 - 1$, and $N/2 = 6893$. I cut off the plot at $f = 30$ day$^{-1}$ (a 48-min period), which is just below the approximate Nyquist critical frequency of the original data, above which there is no additional information.*

Figure 4 shows numerous peaks in the Fourier amplitude over a wide range of frequencies. The magnitude of the Fourier amplitude peaks generally decreases with increasing frequency. Most of the periodicity is concentrated at frequencies below $f = 25$ day$^{-1}$, or at periods longer than one hour. At present, I do not understand the large number of strong Fourier amplitudes

---

*Throughout this work, I use units of day, whose magnitude is given by 1 day = 1 solar day = 1 MJD.
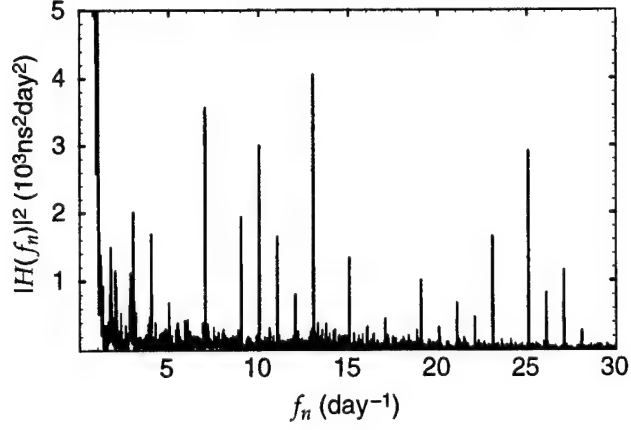
Figure 4: Power spectrum of uniformly resampled data.

in the data. Table 1 lists the prominent peaks in the Fourier amplitudes shown in figure 4. Figure 5 shows the same plot as in figure 4 (on an expanded scale), along with an inset that shows the frequency range $f = 1$ to 8 day$^{-1}$. A strong peak exists at $f = 0.9915644$ day$^{-1}$, which corresponds to a 1.00851-day period. Two much weaker peaks are present at $f = 1.99887$ and 2.01461 day$^{-1}$, which correspond to periods of 0.500283 and 0.496374 day, respectively. To the accuracy of the frequency separations in my Fourier analysis, these periodicities correspond to approximate periods of 1.0 and 0.5 day. The 0.5-day period is close to the average period of the GPS satellites, which is 11.9664 hr = 0.4986 day.* The discrete frequency spacing prevents determination of a more accurate period than is given by the spacing between discrete frequencies.

Figure 6 shows a further expanded scale near $f = 0$. The strongest peak at $f = 0.0157391$ day$^{-1}$ corresponds to the fundamental time period of the data set, $1/f = 63.536$ day. The zero frequency peak represents an overall constant offset of the USNO Master Clock, with respect to GPS time.

---

*The average GPS satellite period 11.9664 hr is an average of the periods of the 25 satellites; data provided by J. Toth and B. Winn of The Aerospace Corporation.

8

Table 1: Frequencies, corresponding periods, and absolute squares of Fourier amplitudes shown for prominent peaks in figures 3–5.

| $f_n$ (day$^{-1}$) | Period (day) | $|H(f_n)|^2$ ($10^3$ ns$^2$ day$^2$) |
|---|---|---|
| 0 | — | 14.4223 |
| 0.0157391 | 63.536 | 808.044 |
| 0.125913 | 7.942 | 36.1935 |
| 0.220348 | 4.53829 | 41.3523 |
| 0.582347 | 1.71719 | 21.8435 |
| 0.629564 | 1.5884 | 19.4908 |
| 0.818434 | 1.22185 | 10.2241 |
| 0.897129 | 1.11467 | 8.31069 |
| 0.991564 | 1.00851 | 25.1686 |
| 1.74704 | 0.572396 | 1.48858 |
| 1.99887 | 0.500283 | 1.14948 |
| 2.01461 | 0.496375 | 1.03249 |
| 2.86452 | 0.349099 | 1.11251 |
| 3.00617 | 0.332649 | 2.00817 |
| 4.01347 | 0.249161 | 1.68535 |
| 5.00504 | 0.199799 | 0.682596 |
| 7.01964 | 0.142457 | 3.56584 |
| 9.01851 | 0.110883 | 1.93372 |
| 10.0258 | 0.0997425 | 3.00274 |
| 11.0331 | 0.0906362 | 1.64622 |
| 12.0404 | 0.0830536 | 0.805485 |
| 13.032 | 0.0767343 | 4.05422 |
| 15.0466 | 0.0664603 | 1.33505 |
| 19.0601 | 0.0524657 | 1.00523 |
| 23.0578 | 0.0433693 | 1.64400 |
| 25.0724 | 0.0398845 | 2.92053 |
| 26.0797 | 0.038344 | 0.821129 |
| 27.0713 | 0.0369395 | 1.14859 |
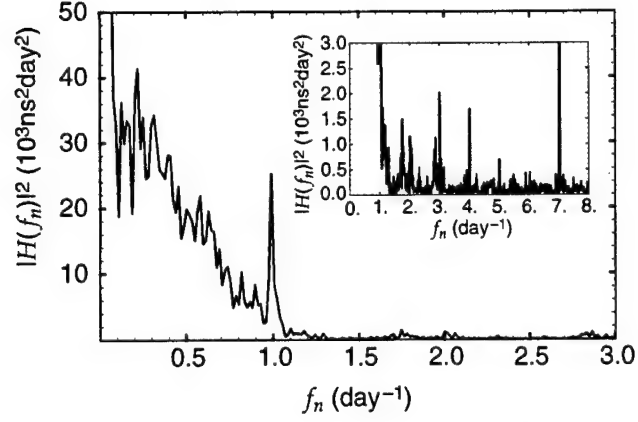
Figure 5: Power spectrum on expanded scale in low-frequency region $f_n = 0$ to 3 day$^{-1}$. (Note: strong peak is seen at $f_n = 0.991564$ day$^{-1}$. Inset shows same spectrum for intermediate frequency region $f = 1$ to 8 day$^{-1}$.)
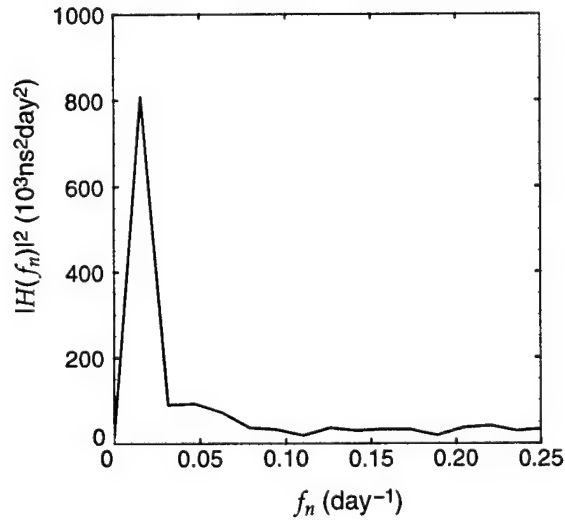


Figure 6: Power spectrum near zero frequency. (Discrete Fourier amplitudes are connected by straight lines.)

10

## 2.2 Correlation Function

In order to determine the periodicity of GPS time more accurately, I computed correlations between successive days of the data. If such correlations exist, they may be due to systematic physical effects, which may warrant further exploration. I designate the original data—that is, the USNO Master Clock time minus the GPS time (plotted in fig. 1)—by the function $f(\tilde{m}_i)$, where $\tilde{m}_i$ are the MJD observation times. In terms of a time variable $t$, these data are given by a function $h(t)$, defined by

$$
\begin{aligned}
f(\tilde{m}) &= h(t) \\
&= h(t_0 + (\tilde{m} + \kappa_0)\Delta t),
\end{aligned}
\tag{4}
$$

where the time $t$ and MJD $\tilde{m}$ are related by

$$
\begin{aligned}
t &= t_0 + \tilde{j}\,\Delta t \\
&= t_0 + (\tilde{m} + \kappa_0)\,\Delta t,
\end{aligned}
\tag{5}
$$

where $\tilde{j}$ is the Julian date [24], $t_0$ is the Julian date epoch (Greenwich mean noon on 1 January 4713 BC), $\kappa_0 = 2400000.5$, and $\Delta t = 1.0$ day. To divide the data into segments of length $T$ and correlate the segments with one another, I introduce the function

$$
\begin{aligned}
h_m(t) &= h(t_0 + (\tilde{m} + \kappa_0)\,\Delta t)\,[\theta(\bar{t}) - \theta(\bar{t} - T)] \\
&= h(t_0 + (m + \kappa_0)\,\Delta t + \bar{t}\,)\,[\theta(\bar{t}) - \theta(\bar{t} - T)],
\end{aligned}
\tag{6}
$$

where $m$ is the integer part of the MJD $\tilde{m}$ that labels the starting time of the data segment, $\bar{t}$ is a shifted time variable such that $\bar{t} = 0$ at the start of the data segment, and $\theta(t) = 1$ for $t \geq 0$ and $\theta(t) = 0$ for $t < 0$. (Note that the function $h_m(t)$ is nonzero only over a time interval of length $T$, which starts at integer MJD $m$.)

For any given day, the mean of the data $f(\tilde{m}_i)$ is not zero. In order to define a normalized correlation function, I define a new function that has zero mean, $e_n(t)$, by subtracting the mean of $h_m(t)$ over the segment of length $T$, so that

$$
e_n(t) = h_n(t) - \langle h_n(t) \rangle,
\tag{7}
$$

where the mean for the data starting on integer MJD $n$ is given by

$$
\langle h_n(t) \rangle = \frac{1}{T} \int_0^T h_n(t)\, dt.
\tag{8}
$$

11

The functions $e_n(t)$ represent the difference data $f(\tilde{m}_i)$ starting on integer MJD $n$, with the mean for that data segment subtracted.

I now define the normalized correlation function between two data segments of length $T$, starting on integer MJD $m$ and MJD $n$, respectively, by

$$g_{m,n}(\tau) = \frac{1}{(N_m \, N_n)^{\frac{1}{2}}} \int_0^T e_m(t) e_n(t - \tau) \, dt, \tag{9}$$

where the normalization constants $N_i$ are given by

$$N_i = \int_0^T e_i^2(t) \, dt. \tag{10}$$

The correlation function in equation (9) is dimensionless and is defined so that, if the time differences $f(\tilde{m}_i)$ are identical for two data segments, $e_m(t) = e_n(t)$, then $g_{m,n}(0) = 1$. An example of the behavior of $g_{m,n}(\tau)$ for a function that is perfectly correlated from one day to another is shown in figure 7, where I calculated the autocorrelation function, $g_{n,n}(\tau)$, of a 1-day segment of data, starting at MJD $n = 50023$. As $\tau \to 0$, the autocorrelation function $g_{n,n}(\tau) \to 1$. For increasing values of $\tau$, $g_{n,n}(\tau)$ decreases for two reasons. First, the data are not correlated at times $\tau > 0$, which leads to a sharp decay of $g_{n,n}(\tau)$. The second reason that $g_{n,n}(\tau)$ decreases for increasing values of $\tau$ is that the functions $e_n(t)$ and $e_n(t - \tau)$ have a decreasing overlap for increasing $\tau$. The finite support (finite nonzero domain) of the function $e_n(t)$ leads to less overlap between $e_n(t)$ and $e_n(t - \tau)$ for $\tau > 0$ than for $\tau = 0$, and leads to the decay of the correlation function $g_{n,n}(\tau)$ for increasing $\tau$. This effect in $g_{n,n+1}(\tau)$ is not significant, since (for example) for two constant functions with finite support, $g_{n,n+1}(\tau)$ would decay approximately linearly with $\tau$, whereas I am interested in sharp peaks in the correlation function (such as the peak near $\tau = 0$ in fig. 7).

From the data, I computed the function $g_{n,n+1}(\tau)$, which is a correlation function between two successive days of the data (that is, I used data segments where $T = 1$ day). When the data on two successive days are completely uncorrelated, we would expect $g_{n,n+1}(\tau)$ for $\tau \sim 0$ to be small. Figures 8 to 10 show the computed correlation functions $g_{n,n+1}(\tau)$ for 25 successive pairs of days in the data. Inspection of each correlation function shows that there is a large systematic correlation near $\tau = 0$ in all cases. The time $\tau = 0$ corresponds to correlations with a period of 24 hr. In principle, it is possible

Figure 7: Autocorrelation function, $g_{n,n}(\tau)$, for $T = 1$ day, from MJD $n = 50023$.
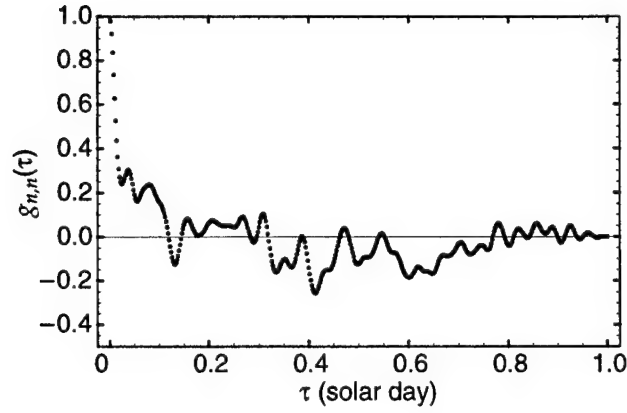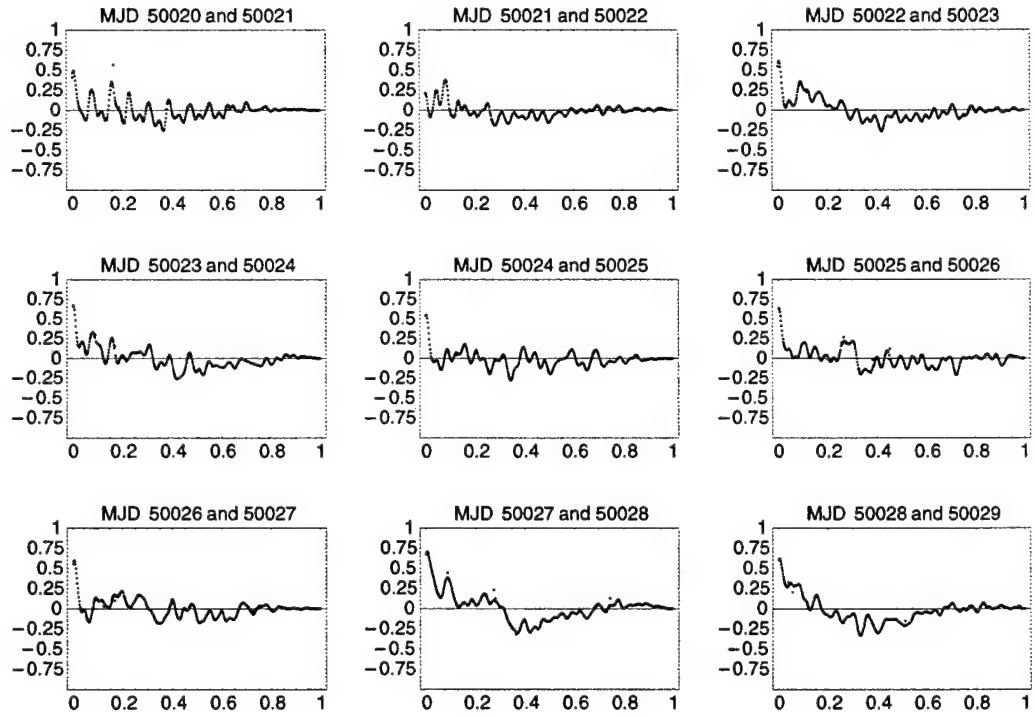


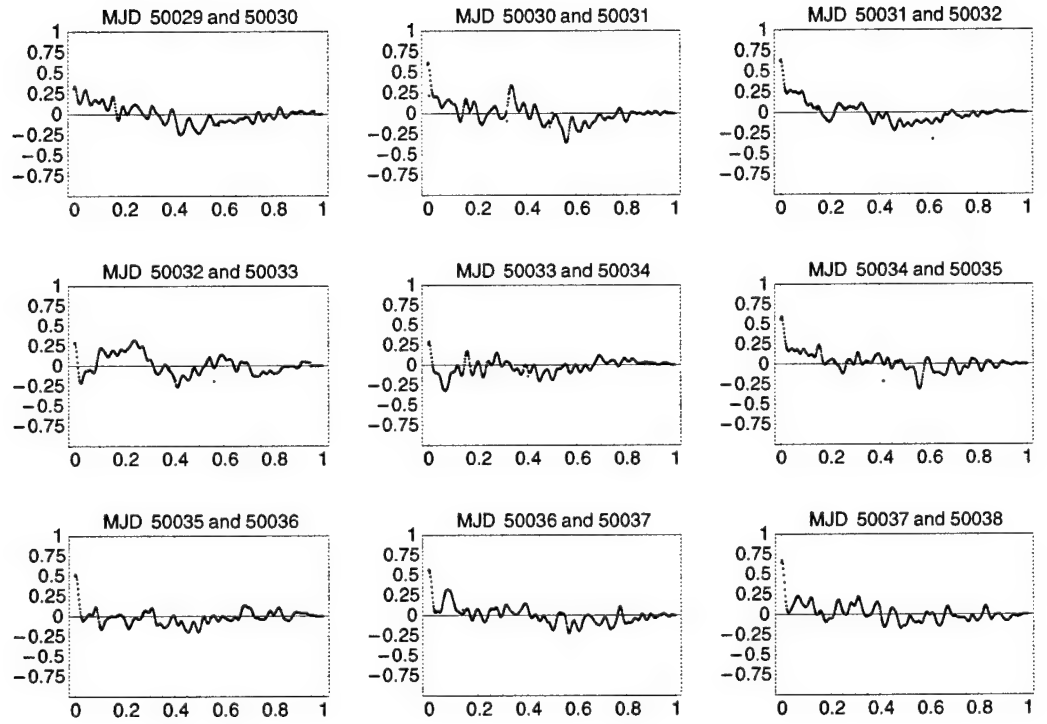Figure 8: Correlation functions, $g_{n,n+1}(\tau)$, for $T = 1$ day, from MJD $n = 50020$ through 50028.

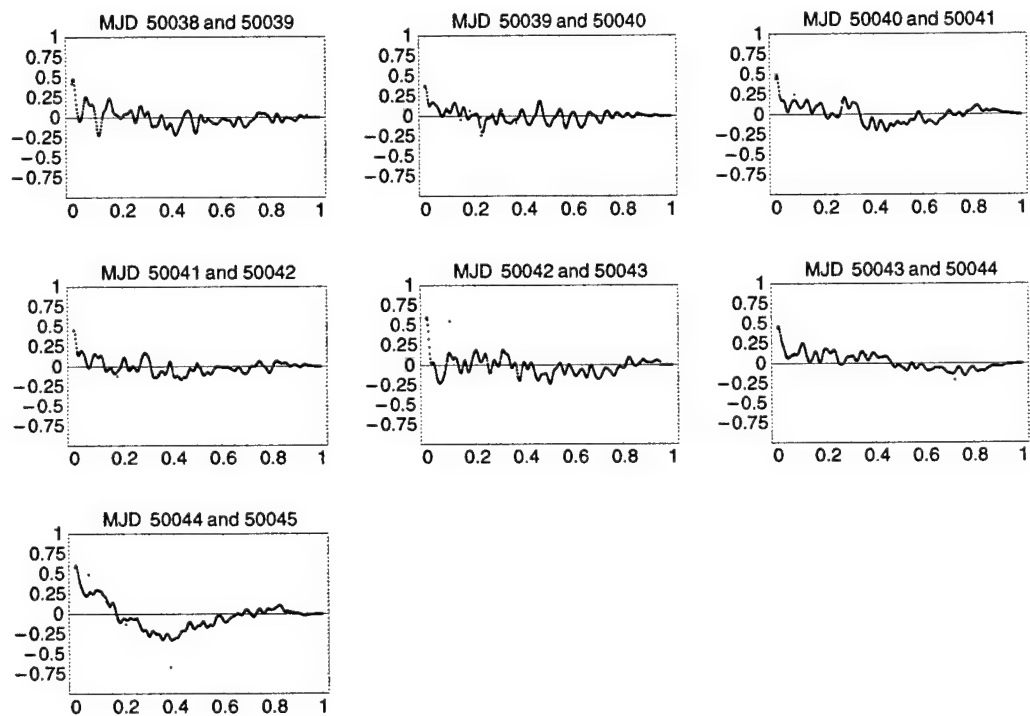Figure 9: Correlation functions, $g_{n,n+1}(\tau)$, for $T = 1$ day, for successive days from MJD 50029 through 50037.

Figure 10: Correlation functions $g_{n,n+1}(\tau)$, for $T = 1$ day, for successive days starting on MJD 50038 through 50044.

15

that a finite sample of 25 successive-day correlation functions might show such correlations even though they do not exist; however, such an event is highly improbable. Figure 11 shows the algebraic average,

$$\langle g_{n,n+1}(\tau) \rangle \quad = \quad \frac{1}{25} \sum_{n=1}^{25} g_{n,n+1}(\tau),\qquad (11)$$

of the 25 correlation functions. This averaging smooths out some of the fluctuations that result from using a finite data set. The averaged correlation function $\langle g_{n,n+1}(\tau) \rangle$ has a peak value of 0.52 at $\tau = 0.0030$ day $\cong 4.32$ min. Since I am taking correlations between successive days, this means that the correlation peaks at 24 hr $-$ 4.32 min, which is in good agreement with the average "24-hr" GPS satellite period—24 hr $-$ 4.032 min.[*]

In the computations above, I computed correlations between two successive days. The results show that there are large correlations at an approximate delay time of 23 hr 56 min, indicating that there is a periodicity in GPS time with respect to the USNO Master Clock, over a one-day time. Using the correlation technique, we can study how long these correlations persist in time. In order to do this, I computed the autocorrelation function $g_{n,n}(\tau)$ (defined in eq (9)) for a 5-day segment of data, $T = 5$ days, from MJD $n = 50020$ to $n = 50025$. This function, $g_{n,n}(\tau)$, is shown in figure 12. Strong peaks

---

[*]The average GPS satellite period 11.9664 hr is an average of the periods of the 25 satellites; data provided by J. Toth and B. Winn of The Aerospace Corporation.
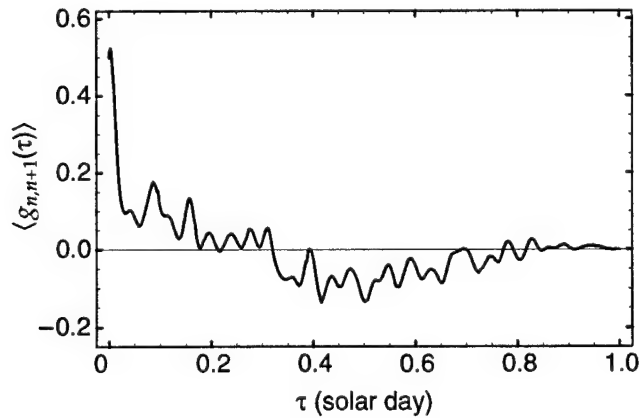


Figure 11: Algebraic average of 25 successive-day correlation functions versus delay time $\tau$.
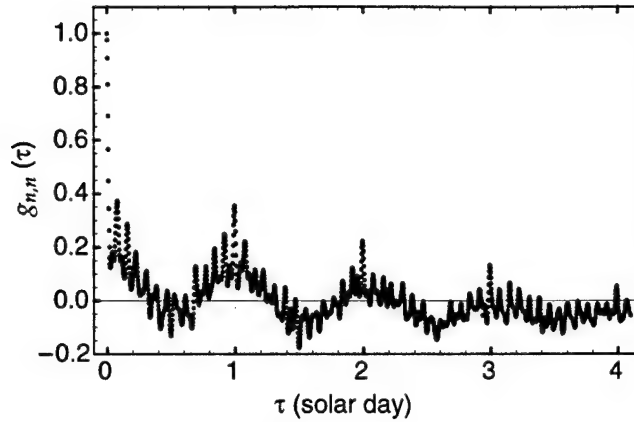
Figure 12: Autocorrelation function, $g_{n,n}(\tau)$, for $T = 5$ days, starting from MJD $n = 50020$ to $50025$, is plotted versus delay time $\tau$. Correlations persist for four successive days.

are seen at approximately 1-day intervals, indicating that the correlation at a delay time of 23 hr 56 min persists for 4 days. This "long-term memory" may be the result of long time constants present in the Kalman filter process, or systematic errors in the GPS.

At present, the source of these effects is unknown, but several sources are possible: incorrect coordinates of the receiver's antenna phase center, errors in the GPS program code, and improper physical models being used to run the system. The strong correlation at the "24-hr" GPS satellite period suggests that some physical effects are at work.

# 3. Summary

The U.S. Naval Observatory Master Clock keeps the official time for DoD. Both the USNO Master Clock and the GPS are intended to keep coordinate time in the ECI (and ECEF) frames of reference [10]. Ideally, both the USNO Master Clock and the GPS are intended to keep the same time scale (modulo leap seconds); hence, if time transfer is done properly, the time difference should be zero or a random function of time with no correlations.

I have obtained time transfer data consisting of the difference between USNO Master Clock time and GPS time. A two-frequency P(Y)-code keyed receiver was used to obtain the data, and the standard two-frequency algorithm was used to correct for ionospheric delay [20].

I computed a Fourier transform of the data. Numerous sharp peaks were evident in the Fourier spectrum. A strong peak in the Fourier amplitude was seen, corresponding to approximately a 24-hr period. Two much weaker peaks were shown, corresponding to approximately 12-hr periods.

In order to determine the period near 24 hr more precisely, I performed a correlation function analysis of the data. A peak occurs in the average correlation function equal to 0.52 at a delay time of 23 hr 56 min, which corresponds to the average "24-hr" GPS satellite period. This large correlation indicates that GPS time, as seen by the U.S. Naval Observatory in time transfer, is periodic with respect to the USNO Master Clock, with period 23 hr 56 min. An autocorrelation of a 5-day segment of data shows that these correlations persisted for four successive days. The observed periodicity in GPS time indicates that there are systematic physical effects that are not adequately modelled in the GPS. Further investigations to determine the origin of these effects may lead to an improvement in overall GPS performance.

# Acknowledgments

# Bibliography

1. B. W. Parkinson and J. J. Spilker, eds., *Global Positioning System: Theory And Applications*, vol. I and II (P. Zarchan, editor-in-chief), Progress in Astronautics and Aeronautics, vol. 163 and 164, Amer. Inst. Aero. Astro., Washington, DC (1996).

2. Committee on the Future of the Global Positioning System, *The Global Positioning System: A Shared National Asset, Recommendations for Technical Improvements and Enhancements*, Commission on Engineering and Technical Systems, National Research Council, National Academy Press, Washington, DC (1995).

3. B. Hofmann-Wellenhof, H. Lichtenegger, and J. Collins, *Global Positioning System Theory and Practice*, Springer-Verlag, New York (1993).

4. E. D. Kaplan, *Understanding Principles and Applications*, Mobile Communications Series, Artech House, Boston (1996).

5. W. E. Howard, whitepaper study, "The Evolution of GPS Accuracy: Implications for Army Operations" (1995, unpublished).

6. R. Loh, "Seamless Aviation: FAA Wide Area Augmentation System," *GPS World* **6**, No. 4 (1995).

7. N. Ashby and D. W. Allan, *Radio Sci.* **14** (1979), 649.

8. K. R. Brown, Jr.,"The Theory of the GPS Composite Clock," *Inst. Navigation GPS-91 Conf. Proc.* (1991), p 223.

9. P. S. Jorgensen, "Relativity Correction in GPS User Equipment," IEEE Position and Navigation Symp., Las Vegas, NV (November 1986).

10. N. Ashby, "A Tutorial on Relativistic Effects in the Global Positioning System," report on NIST contract 40RANB9B8112 (February 1990); *Chin. J. Syst. Eng. Elect.* **6** (1995), 199.

11. N. Ashby and J. J. Spilker, in *Global Positioning System: Theory And Applications*, vol. I and II, B. W. Parkinson and J. J. Spilker, eds. (P. Zarchan, editor-in-chief), Progress in Astronautics and Aeronautics, vol. 163 and 164, Amer. Inst. Aero. Astro., Washington, DC (1996).

12. J. J. Spilker, Jr., "GPS Signal Structure and Performance Characteristics," *Navigation J. Inst. Navigation* **25**, No. 2 (1978), 121.

13. S. A. Klioner, *Celest. Mechan. Dynam. Astron.* **53** (1995), 81.

14. G. Petit and P. Wolf, *Astron. Astrophys.* **286** (1994), 971.

15. G. Petit and P. Wolf, *Astron. Astrophys.* **304** (1995), 653.

16. TOPEX/POSEIDEN Project, *Global Positioning System (GPS) Precise Orbit Determination (POD) Software Design*, Jet Propulsion Laboratory, JPL D-7275 (9 March 1990).

17. R. A. Nelson, "An Analysis of General Relativity in the Global Positioning System Time Transfer Algorithm," report prepared for the U.S. Naval Research Lab., contract N00014-90-C-2074 (September 1991), pp 91–93.

18. M. Weiss, "Apparent Diurnal Effects in the Global Positioning System," *Proc. Nineteenth Annual Precise Time and Time Interval (PTTI) Appl. Planning Meeting,* Redondo Beach, CA (December 1987).

19. T. B. Bahder, *Correlations Between GPS and USNO Master Clock Times*, GPS Performance Analysis Working Group, Falcon Air Force Base, CO (August 1995); also presented at "GPS for Land Combat Applications" Army workshop, University of North Carolina (August 1995).

20. Navstar GPS Space Segment/Navigation User Interfaces, ICD-GPS-200, Revision C, Arinc Research Corporation (10 October 1993).

21. M. Miranian, *UTC Dissemination to the Real-Time User: The Role of USNO*, 27th Annual Precise Time and Time Interval (PTTI) Applications Planning Meeting, 29 November to 1 December 1995, San Diego, California.

22. Mihran Miranian and William J. Klepczynski, "Time Transfer via GPS at USNO," *Institute of Navigation GPS-91 Conference Proceedings* (1991).

23. W. H. Press, S. A. Teukolsky, W. T. Vetterling, and B. Flannery, *Numerical Recipes in C: the Art of Scientific Computing*, 2nd edition, Cambridge University Press, New York, New York (1992).

24. P. K. Seidelmann, ed., *Explanatory Supplement to Astronomical Almanac*, University Science Books, Mill Valley, CA (1992).

# Distribution

Admnstr
Defns Techl Info Ctr
Attn DTIC-OCP 1
8725 John J Kingman Rd Ste 0944
FT Belvoir VA 22060-6218

Defns Mapping Agency
Attn R Klotz
4211 Briars Rd
Olney MD 20832-1814

Defns Mapping Agency
Attn L-A1 B Tallman
Attn L-41 D Morgan
Attn L-41 F Mueller
Attn L-41 B Hagan
3200 2nd Stret
ST Louis MO 63116

Defns Mapping Agency Sys Ctr
Attn Code SC/Eid S Malys MS D-84
4600 Sangamore Rd
Bethesda MD 20816-5003

Ofc of the Secy of Defs
Attn ODDRE (R&AT) G Singley
Attn ODDRE (R&AT) S Gontarek
The Pentagon
Washington DC 20301-3080

AMC OMP/746 TS
Attn A Chasko
PO Box 310
High Rolls NM 88325

Army Rsrch Ofc
Attn B Gunther
Attn H Everitt
Attn M Stroscio
Attn G Iafrate
Attn AMXRO-PH D Skatrud
4300 S Miami Blvd
Research Triangle Park NC 27709

CECOM
Attn PM GPS COL S Young
FT Monmouth NJ 07703

CECOM RDEC
Cmnd & Cntrl Sys Integration Dirctrt
Attn AMSEL-RD-C2-ES P Olson Bldg 2525
FT Monmouth NJ 07703

CECOM RDEC Electronic Systems Div Dir
Attn J Niemela
FT Monmouth NJ 07703

CECOM
Sp & Terrestrial Commctn Div
Attn AMSEL-RD-ST-MC-M H Soicher
FT Monmouth NJ 07703-5203

DARPA
Attn B Kaspar
Attn J Pennella
Attn L Stotts
3701 N Fairfax Dr
Arlington VA 22203-1714

Dpty Assist Scy for Rsrch & Techl
Attn SARD-TR R Chait
Attn SARD-TT D Chait
Attn SARD-TT F Milton Rm 3E479
Attn SARD-TT K Kominos
Attn SARD-TT R Reisman
Attn SARD-TT T Killion
The Pentagon Rm 3E476
Washington DC 20310-0103

DUSD Space
Attn 1E765 J G McNeff
3900 Defense Pentagon
Washington DC 20301-3900

MICOM RDEC
Attn AMSMI-RD W C McCorkle
Attn AMSMI-RD-MG-NC A Killen
Attn AMSMI-RD P Jacobs
Redstone Arsenal AL 35898-5240

MICOM RDEC Weapons Sci Dirctrt
Attn J Dowling
Redstone Arsenal AL 35898-5240

# Distribution

OSD
Attn OUSD(A&T)/ODDDR&E(R)  J  Lupo
The Pentagon
Washington DC 20301-7100

US Army Matl Cmnd
Dpty CG for RDE Hdqtrs
Attn AMCRD  BG  Beauchamp
5001 Eisenhower Ave
Alexandria VA 22333-0001

US Army Matl Cmnd
Prin Dpty for Acquisition Hdqrts
Attn AMCDCG-A  D  Adams
5001 Eisenhower Ave
Alexandria VA 22333-0001

US Army Matl Cmnd
Prin Dpty for Techlgy Hdqrts
Attn AMCDCG-T  M  Fisette
5001 Eisenhower Ave
Alexandria VA 22333-0001

US Army MICOM
Attn AMSMI-RD-MG-NC  G  Graham
Redstone Arsenal AL 35898-5254

US Army MICOM RDEC
Attn B  Baeder
Bldg 5400
Redstone Arsenal AL 35898

USAASA
Attn MOAS-AI  W  Parron
9325 Gunston Rd Ste N319
FT Belvoir VA 22060-5582

Nav Rsrch Lab
Attn C  Gilbreath
Attn Code 8150  R  Beard
Attn W  Reid
Attn Code 8150/SFA  J  Buisson
4333 Overlook Ave SW
Washington DC 20375

Nav Surface Warfare Ctr
Attn Code K12  E  Swift
Attn G  Wiles
Attn Code K12  J  O'Toole
17320 Dahlgren Rd
Dahlgren VA 22448-5100

NAVSTAR GPS JPO
Attn SMC/CZJ  D  Crane
2435 Vela Way, Ste 1613
Los Angeles AFB CA 90245-5500

Ofc of Nav Rsrch
Attn ONR 331  H  Pilloff
800 N Quincy Stret
Arlington VA 22217

US Nav Obs Time Services Dept
Attn F  Vannicola
Attn M  Miranian
3450 Massachuetts Ave
Washington DC 20392-5420

US Nav Observatory
Alternate Master Clock
Attn S Hutsell
400 O'Malley Ave Ste 44
Falcon AFB CO 80912-4044

US Nav Observatory
Attn K  Johnston
3450 Massachusetts Ave NW
Washington DC 20392-5240

US Nav Observatory
Attn B  Bollwerk
5580 Piedra Vista
Colorado Springs CO 80908

AFSPC/DRFN
Attn CAPT R  Koon
150 Vandenberg Stret Ste 1105
Peterson AFB CO 80914-45900

Air Force Phillips Lab
Attn GPIM  J A  Klobuchar
29 Candolf Rd
Hanscom AFB MA 01731-3010

ASC OL/YUH
Attn JDAM-PIP  LT V  Jolley
102 W D Ave
Eglin AFB FL 32542

DOT AFSPC/DRFN
Attn H  Skalski
150 Vandenberg Stret
Peterson AFB CO 80914

# Distribution

GPS Joint Prog Ofc Dir
Attn COL J Clay
2435 Vela Way Ste 1613
Los Angeles AFB CA 90245-5500

Holloman AFB
Attn K Wernie
1644 Vandergrift Rd
Holloman AFB NM 88330-7850

Ofc of the Dir Rsrch and Engrg
Attn R Menz
Pentagon Rm 3E1089
Washington DC 20301-3080

Special Assist to the Wing Cmndr
Attn 50SW/CCX CAPT P H Bernstein
300 O'Malley Ave Ste 20
Falcon AFB CO 80912-3020

USAF SMC/CED
Attn DMA/JPO M Ison
2435 Vela Way Ste 1613
Los Angeles AFB CA 90245-5500

NIST
Attn MS 847.5 M Weiss
Attn S Jefferts
325 Broadway
Boulder CO 80303

Space Environment Lab/NOAA
Attn R/E/SE J Kunches
325 Broadway
Boulder CO 80303

Space Geodesy Br
Attn E C Pavlis
Attn J Bosworth
Greenbelt MD 20771

Applied Rsrch Lab Univ of Texas
Attn B Renfro
Attn J Saunders
Attn R Mach
PO Box 8029
Austin TX 78713-8029

ARL Electromag Group
Attn Campus Mail Code F0250 A Tucker
University of Texas
Austin TX 78712

Stanford University
Attn HEPL/GP-B D Lawrence
Attn HEPL/GP-B T Walter
Stanford CA 94305-4085

Univ of Colorado
Dept of Physics
Attn N Ashby
Campus Box 390
Boulder CO 80309-0390

Univ of Maryland
Dept of Physics
Attn C Alley
Attn T Van Flandern
Attn C W Misner
College Park MD 20742

Aerospace
Attn J Langer
Attn M4/954 C Yinger
Attn M Dickerson
PO Box 92957 M4/954
Los Angeles CA 90009

Aerospace Corp
Attn MS M4-944 J Toth
Attn A Wu MS M5/686
Attn B Feess MS M4/956
Attn B Winn MS M5/685
Attn H F Fliegel MS M5/685
Attn R DiEsposti
Attn A Satin
2350 E El Segundo Blvd
El Segundo CA 90245

Allen's Time
Attn D Allan
PO Box 66
Fountain Green UT 84632

# Distribution

ARINC
Attn L  Conover
1925 Aerotech Dr Ste 212
Colorado Springs CO 80916

ARINC
Attn P  Mendoza
4055 Hancock Stret
San Diego CA 92110

Ashtech Inc
Attn S  Gourevitch
1177 Kifer Rd
Sunnyvale CA 94086

ATA Assoc
Attn M  Harkins
6800 Backlick Rd
Springfield VA 22150

BD Systems
Attn J  Butts
385 Van Ness Ave #200
Torrance CA 90501

Charles Stark Draper Lab
Attn R  Greenspan
555 Technology Sq
Cambridge MA 02139-3563

Hewlett-Packard Co
Attn J  Kusters
5301 Stevens Creed Blvd
Santa Clara CA 95052

Hughes
Attn S  Peck
Attn R  Malla
800 Apollo Ave PO Box 902
El Segundo CA 90245

Hughes Space & Comm
Attn MS/SC/SIO/S364  C  Shecklells
PO Box 92919 Airport Station
Los Angeles CA 90009

Intermetrics Inc
Attn J  McGowan
615 Hope Rd Bldg 4 2nd floor
Eatontown NJ 07724

ITT Aerospace
Attn MS 2511  R  Peller
Attn MS 8528  H  Rawicz
Attn MS 8538  L  Doyle
Attn P  Brodie
100 Kingsland Rd
Clifton NJ 07014

KERNCO
Attn R  Kern
28 Harbor Stret
Danvers MA 01923

Lockheed Martin
Attn J  Taylor
Attn B  Marquis
1250 Academy Park Loop Ste 101
Colorado Springs CO 80910

LORAL
Attn B  Mathon
Attn 182/3N73  D H  Winfield
Attn S  Francisco Bldg 182/3A60
700 N Frederick Pike
Gaithersburg MD 20879

LORAL
Attn B  Pisor
2915 Baseline Rd #530
Boulder CO 80303

LORAL Federal Systems
Attn J  Kane
Attn M  Baker
Attn R  Astalos
9970 Federal Dr
Colorado Springs CO 80921

Magnavox Electric Sys Company
Attn D  Thornburg
2829 Maricopa Stret
Torrance CA 90503

# Distribution

Overlook Systems
Attn D Brown
Attn T Ocvirk
1150 Academy Park Loop Ste 114
Colorado Springs CO 80910

PAQ Commctn
Attn Q Hua
607 Shetland Ct
Milpitas CA 95035

Rockwell CACD
Attn L Burns
400 Collins Rd NE
Cedar Rapids IA 52398

Rockwell Collins
Attn C Masko
Cedar Rapids IA 52498

Rockwell DA85
Attn W Emmer
12214 Lakewood Blvd
Downey CA 92104

Rockwell Space Ops Co
Attn AFMC SSSG DET2/NOSO/Rockwell
  R Smetek
Attn B Carlson
442 Discoverer Ave Ste 38
Falcon AFB CO 80912-4438

Rockwell Space Systems Div
Attn Mailcode 841-DA49 D McMurray
12214 Lakewood Blvd
Downey CA 90241

SRI
Attn M/S BS378 M Moeglein
333 Ravenswood Ave
Menlo Park CA 94025

Stanford Telecom
Attn B F Smith
1221 Crossman Ave
Sunnyvale CA 94088

Surveying Div
Attn CETEC-TD-GS D C Oimoen
7701 Telegraph Rd
Alexandria VA 22315-3864

TASC
Attn T Bartholomew
1190 Winterson Rd
Linthicum MD 21090

Trimble Nav
Attn L Kruczynski
Attn P Turney
585 N Mary
Sunnyvale CA 94086

Army Rsrch Lab
Attn AMSRL-PS-ED J Vig
FT Monmouth NJ 07703

Army Rsrch Lab
Attn AMSRL-D J Lyons
Attn AMSRL-SE-EM G Simonis
Attn AMSRL-SE-EM J Bruno
Attn AMSRL-SE-EM R Leavitt
Attn AMSRL-SE-EP D Wortman
Attn AMSRL-CI-LL Tech Lib (3 copies)
Attn AMSRL-CS-AL-TA Mail & Records
  Mgmt
Attn AMSRL-CS-AL-TP Techl Pub (3 copies)
Attn AMSRL-SE-EA J Eicke
Attn AMSRL-SE-EM T B Bahder (15 copies)
Attn AMSRL-SE-IS V DeMonte
Adelphi MD 20783-1197

# REPORT DOCUMENTATION PAGE

Form Approved
OMB No. 0704-0188

Public reporting burden for this collection of information is estimated to average 1 hour per response, including the time for reviewing instructions, searching existing data sources, gathering and maintaining the data needed, and completing and reviewing the collection of information. Send comments regarding this burden estimate or any other aspect of this collection of information, including suggestions for reducing this burden, to Washington Headquarters Services, Directorate for Information Operations and Reports, 1215 Jefferson Davis Highway, Suite 1204, Arlington, VA 22202-4302, and to the Office of Management and Budget, Paperwork Reduction Project (0704-0188), Washington, DC 20503.

| 1. AGENCY USE ONLY (Leave blank) | 2. REPORT DATE<br>June 1997 | 3. REPORT TYPE AND DATES COVERED<br>Final, from November 1995 to May 1997 |
|---|---|---|

**4. TITLE AND SUBTITLE**
Correlations between Global Positioning System and U.S. Naval Observatory Master Clock Time

**5. FUNDING NUMBERS**
DA PR: 6.27.05.AH94
PE: 622705.H9411

**6. AUTHOR(S)**
Thomas B. Bahder

**7. PERFORMING ORGANIZATION NAME(S) AND ADDRESS(ES)**
U.S. Army Research Laboratory
Attn: AMSRL-SE-EM
2800 Powder Mill Road
Adelphi, MD 20783-1197

**8. PERFORMING ORGANIZATION REPORT NUMBER**
ARL-TR-1282

**9. SPONSORING/MONITORING AGENCY NAME(S) AND ADDRESS(ES)**
MICOM RDEC
Bldg 5400
Red Arsenal, AL 35898-5240

**10. SPONSORING/MONITORING AGENCY REPORT NUMBER**

**11. SUPPLEMENTARY NOTES**
AMS code: 622705.H9411
ARL PR: 6EFA71

**12a. DISTRIBUTION/AVAILABILITY STATEMENT**
Approved for public release; distribution unlimited.

**12b. DISTRIBUTION CODE**

**13. ABSTRACT** (Maximum 200 words)

The U.S. Naval Observatory Master Clock is used to steer Global Positioning System (GPS) time. Time-transfer data consisting of the difference between the Master Clock time and the GPS time were recorded from all satellites in the GPS constellation over a time period covering 10 October to 12 December 1995. A Fourier analysis of these data shows a distinct peak in the Fourier spectrum, corresponding approximately to a one-day period. For a more accurate determination of this period, correlations are computed between successive days of data. An average of 25 correlation functions shows a correlation equal to 0.52 at a delay time of 23 hr 56 min (which corresponds to twice the average GPS satellite period). This correlation indicates that GPS time, as measured by the U.S. Naval Observatory, is periodic with respect to the Master Clock, with a period of 23 hr and 56 min. An autocorrelation of a five-day segment of data indicates that these correlations persist for four successive days.

**14. SUBJECT TERMS**
GPS, time transfer, satellite, timescale, diurnal variation, atomic clocks, position determination

**15. NUMBER OF PAGES**
29

**16. PRICE CODE**

| 17. SECURITY CLASSIFICATION OF REPORT<br>Unclassified | 18. SECURITY CLASSIFICATION OF THIS PAGE<br>Unclassified | 19. SECURITY CLASSIFICATION OF ABSTRACT<br>Unclassified | 20. LIMITATION OF ABSTRACT<br>UL |
|---|---|---|---|

NSN 7540-01-280-5500

Standard Form 298 (Rev. 2-89)
Prescribed by ANSI Std. Z39-18
298-102

29